Proceedings of the 7th International Conference of Recent Trends in Environmental Science and Engineering (RTESE'23)
Canada – June 04 - 06, 2023
Paper No. 143
DOI: 10.11159/rtese23.143

A Single-Step Synthesis of Defective Graphitic Carbines from Melamine and Urea for Photocatalytic Applications

Beenish Tahir [1], Mohamed A. Hamouda [1,2], Ashraf Aly Hassan [1,2]
[1]Department of Civil and Environmental Engineering, College of Engineering, United Arab Emirates University, P.O.BOX 15551. United Arab Emirates
[2]National Water and Energy Center, United Arab Emirates University, Al Ain P.O. Box 15551, United Arab Emirates
Beenish.t@uaeu.ac.ae; m.hamouda@uaeu.ac.ae; alyhassan@uaeu.ac.ae

Abstract –Recently, there has been a growing interest in relying on photocatalytic technology for producing renewable fuels such as hydrogen and other environmental applications. The success of photocatalysis, however, requires developing visible light-responsive photocatalysts for the continuous production of H_2 and other value-added chemicals. Graphitic carbon nitride (g-C_3N_4) is a promising material but has diminished photocatalytic ability. This work aims to design and develop visible light responsive g-C_3N_4 using a single-step hydrothermal approach. The g-C_3N_4 was prepared through the thermal decomposition of melamine (named g-C_3N_4-M), urea (named g-C_3N_4-U), and a mixture of melamine-urea (named g-C_3N_4-MU). The samples were characterized using X-ray diffraction (XRD), UV-visible, and photoluminescence to assess the successful conversion to g-C_3N_4. XRD results revealed that urea was not successfully converted to g-C_3N_4; however, melamine was fully converted to g-C_3N_4. Interestingly, when melamine and urea were mixed as a fixed bed, the mix was successfully converted to defective g-C_3N_4. Visible light responsiveness was confirmed by the results of UV-visible analysis for all three materials. In the case of melamine, a higher visible light response was obtained (~482 nm), whereas g-C_3N_4-MU had slightly lower visible light absorption (~ 471 nm) due to the interaction of defects within the surface. These findings were further confirmed through photoluminescence analysis. The highest charge carrier recombination was obtained using g-C_3N_4-M, whereas charge separation was improved in the g-C_3N_4-U sample due to the presence of g-C_3N_4 composites and other intermediates. The highest charge separation ability was achieved for the g-C_3N_4-MU. This revealed that mixing melamine and urea is a promising approach for the single-step synthesis of defective g-C_3N_4 with a higher ability for visible light absorption and photoinduced charge carrier separation. The findings of this work would be beneficial in different areas, such as solar energy conversion, greenhouse gas reduction, and wastewater degradation.

***Keywords*:** Synthesis; Melamine; Urea; Characterization; Photocatalyst; Graphitic Carbon nitride

1. Introduction

The recent energy crisis and environmental pollution have significantly impacted human health and the environment. These issues are directly related to the rapid growth of the world population and the consequent increase in urbanization and industrialization. To combat the environmental pressures resulting from this growth, technologies for pollution removal and environmental protection have steadily taken top priority. A promising technology is that of heterogeneous photocatalysis, mainly due to its direct use of solar energy in its activation for different applications. Its success in reducing environmental contaminants has raised interest in environmental remediation [1]. However, several challenges hinder mainstreaming the application of photocatalysis. These challenges include the poor photocatalytic efficiencies of previously developed photocatalysts and the high cost of heterogeneous photocatalysts when considered for large-scale practical applications. Moreover, some attempts to implement heterogeneous photocatalysis in environmental remediation did not yield the desired results [2]. This has prompted researchers to develop new photocatalytic materials that overcome these challenges.

Among the materials investigated for photocatalytic applications, graphitic carbon nitrides (g-C_3N_4) are promising for their suitable band structures and lower tolerable band gap energy for full light utilization [3]. As a noble metal-free material, g-C_3N_4 is gaining popularity among scientists. It offers several advantages, including chemical and thermal stability, affordability, the potential for negative reduction, and the capacity to run on solar energy [4, 5]. However, it has significant drawbacks, such as a small, exposed surface area, a compact layered structure, and a greater rate of photoinduced charge carrier recombination [6, 7].

The photoactivity of g-C_3N_4 can be enhanced through several methods, such as metal loading and coupling with other semiconductors. However, these methods are uneconomical and expensive. Several methods were recently investigated to produce g-C_3N_4 higher performance without further modification. Inducing surface defects and alteration in surface

morphology are among the promising approaches [8]. Surface defects can alter the structure and morphology, preventing charges from recombining and releasing additional active sites [9, 10]. Recently, it was reported that structural surface defects significantly decrease photoinduced charge carrier recombination and boost the mobility of electrons inside the layered surface [11, 12]. Numerous surface-active sites are present in the porous structure of g-C_3N_4, which considerably increases photoactivity [13]. From this perspective, g-C_3N_4 microrods with surface-level C and N dual vacancies are advantageous for fostering photocatalytic organic pollutant removal and H_2O_2 synthesis [14]. Other advantages of g-C_3N_4, such as possessing more excited electrons, more channels inside the heterostructure, and improved light transmission ability, can help a photocatalytic process. The catalyst synthesis procedures have a considerable impact on production costs, photocatalytic performance, and impact on the environment. Several approaches were investigated to induce surface defects in g-C_3N_4 one alternative is the hydrothermal technique which was used to create 3D macroporous g-C_3N_4 using SiO_2 as a template. The resulting increased photocatalytic activity was caused by better light use and favourable mass transfer [15]. Other attempts include the production of 3D g-C_3N_4 with a carbon vacancy using polymethylmethacrylate (PMMA) spheres, which resulted in higher H_2 production than that from bulk g-C_3N_4 [16]. Similarly, 3D g-C_3N_4 was created using microwave vibration and doping with Cu and WO_3 to increase the rate of H_2 production [17].

Although, there has been growing research on the synthesis of different types of g-C3N4 nanotextures, however, expensive routes were adopted. In this work, the single step synthesis of defective graphitic carbon nitride was assisted using melamine and urea precursors. A hydrothermal process was used to achieve a good morphology with bigger active surface, greater light penetration, and better charge carrier separation. For this purpose, three different samples using melamine, urea and mixture of melamine-urea were synthesized and their performance was compared based on light absorption and charge separation ability.

2. Materials and Methods

2.1. Synthesis of Graphitic Carbide Nitride

For the synthesis of graphitic carbon nitride (g-C3N4), melamine (99%, Sigma Aldric, Germany) and Urea (Merck, 99.9 %, Germany) were used as the precursors. The graphitic carbon nitride was synthesized using melamine and urea as the precursors. For the synthesis of bulk graphitic carbon nitride (g-C3N4-M), melamine was used as the precursor. Briefly, melamine powder (5 g) was placed in a covered alumina crucible and thermally treated at 550 ℃ for 2 h in a muffle furnace. After completing the process, the bulk material was grinded to fine powder using piston and mortal and was named graphitic carbon synthesized from melamine (g-C3N4-M). The schematic illustration for the synthesis of g-C3N4-M is presented in Fig. 1 (a).

The g-C3N4 nanosheets were prepared by the thermal decomposition of urea as the precursor. A specific amount of urea (5 g) was placed in a ceramic crucible and was heated in a muffle furnace at 550 ℃ for 2 hours. After cooling to room temperature, the yellowish cake was ground to a fine powder and was named urea-assisted graphitic carbon nitride (g-C3N4-U). The schematic illustration for the synthesis of g-C3N4-U is presented in Fig. 1 (b).

The defective graphitic carbon nitride samples were synthesized using a hydrothermal approach. The defective g-C3N4 was synthesized using a mixture of melamine and urea, in which the sample was heated at 550 ℃ with a total time of 2 h. Urea and melamine were added to the fixed bed and were covered with a lid to minimize exposure to air. The final bulk product has a porous structure and was ground to fine powder and was named defective g-C3N4-MU. The schematic illustration for the synthesis of g-C3N4-MU is presented in Fig. 1 (c)

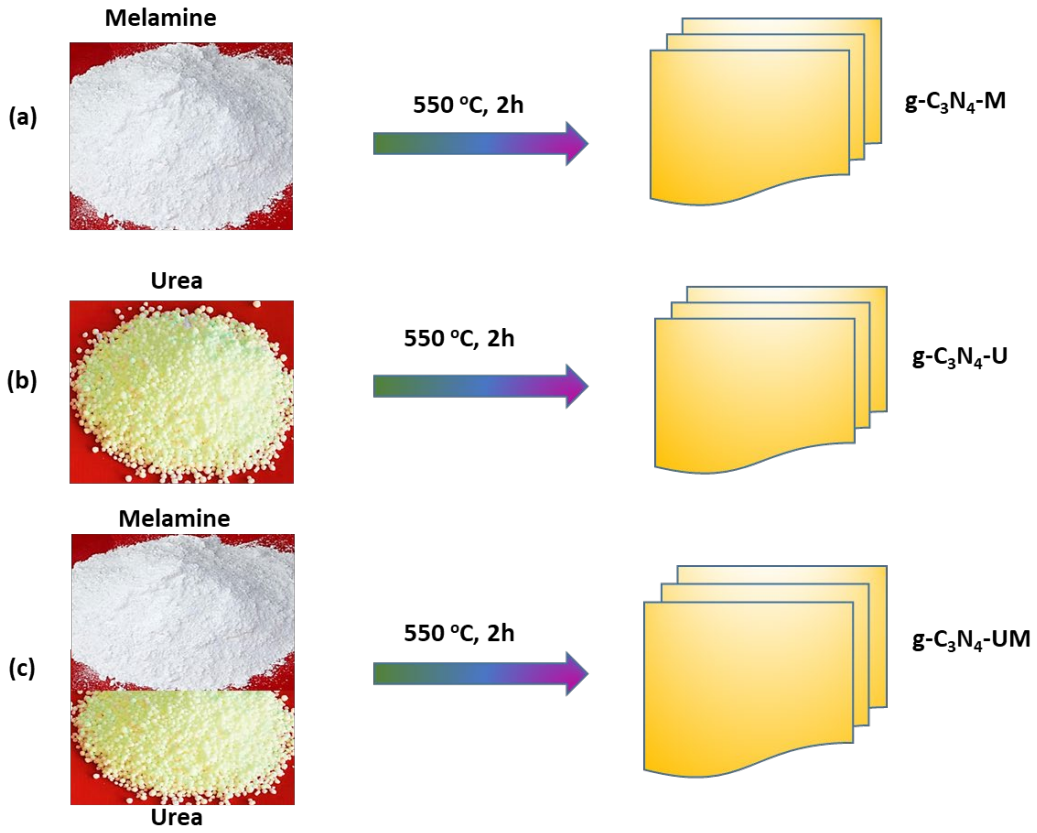

Fig. 1: Schematic illustration for the synthesis of graphitic carbon nitride from different precursors: (a) synthesis of g-C_3N_4 using melamine (g-C_3N_4-M), (b) synthesis of g-C_3N_4 using urea (g-C_3N_4-M) and (c) synthesis of g-C_3N_4 using a mixture of melamine-urea (g-C_3N_4-MU).

2.2. Material Characterization

The structure, crystallinity, light absorption, and capacity for the charge separation of the material were studied using several instruments. The Bruker Advance D8 diffractometer was used for the XRD investigation to identify the crystalline structure. Photoluminescence analysis was then carried out using a spectrometer from HORIBA Scientific (laser 632 nm). Using the UV-3600 Plus Spectrometer, the band gap energy and light absorption were estimated.

3. Results and Discussion

3.1. XRD Analysis

Fig. 2 shows XRD patterns of the g-C_3N_4-M, g-C_3N_4-U, and g-C_3N_4-MU samples to understand their crystalline structure and phase composition. For the case of g-C_3N_3-M, in contrast to the peaks seen at 2θ of 13.12°, which is related to (1 0 0) crystal planes of g-C_3N_4, the strong peak at 2θ of 27.61° reflects the (0 0 2) crystal plane of g-C_3N_4 comprising typical aromatic ring with interlayers [12]. Furthermore, g-C_3N_4 synthesized using urea (g-C_3N_4-U) has several peaks. Two peaks at 12.80° and 26.94° belongs to pure g-C_3N_4 with a crystalline structure and have the same reflections as the g-C_3N_4-M. The other peaks at 2θ of 36.70°, 42.95°, 63.31° and 76.40° belong to the unconverted urea and intermediate structures of g-C_3N_4 instead of pure polymeric structure. More interestingly, pure g-C_3N_4 was obtained when the melamine and the urea were decomposed under the same thermal conditions. This reveals that urea was useful for exfoliating g-C_3N_4 structure and produces defects that would be promising to promote photoinduced charge carrier separation. This also demonstrates that the crystal structure of g-C_3N_4 was unaffected by synthesizing in a single step [18]. Additionally, few other impurity peaks

were found, which would be responsible for creating defects inside the g-C_3N_4 structure. This is in agreement with results reported in earlier literature [15].

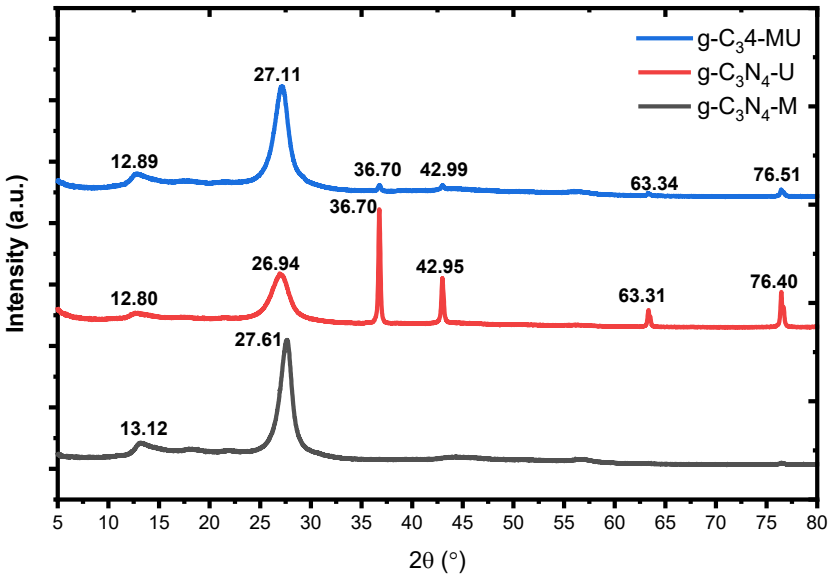

Fig. 2: XRD patterns of g-C_3N_4-M, g-C_3N_4-U, and g-C_3N_4-MU samples.

3.2. UV-visible Analysis

Using UV-visible diffuse reflectance spectra (DRS), the light absorption ability of g-C_3N_4-M, g-C_3N_4-U, and g-C_3N_4-MU was estimated, and the findings are shown in Fig. 3. All the samples exhibit light absorption in the visible light region; however, the trends were different for different samples. The light absorption of 451nm, 471 nm, and 482 nm were obtained for g-C_3N_4-U, g-C_3N_4-MU, and g-C_3N_4-M samples, respectively. The sample synthesized using urea (g-C_3N_4-U) has lower light absorption compared to g-C_3N_4-M synthesized using melamine. This was due to the higher quality of g-C_3N_4 obtained with melamine as a precursor compared to urea. Comparatively, samples synthesized using a mix of melamine and urea had light absorption than that using only urea as a precursor. Nevertheless, they were still lower than those obtained when only melamine was used as a precursor. This was possibly due to the creation of defective g-C_3N_4 with a covered interface structure and reduced light absorption ability [12]. The different levels of light absorption could also be due to variations in the forms and morphologies of the three samples. In general, all the samples have light absorption within the visible light range and can be employed for solar energy applications.

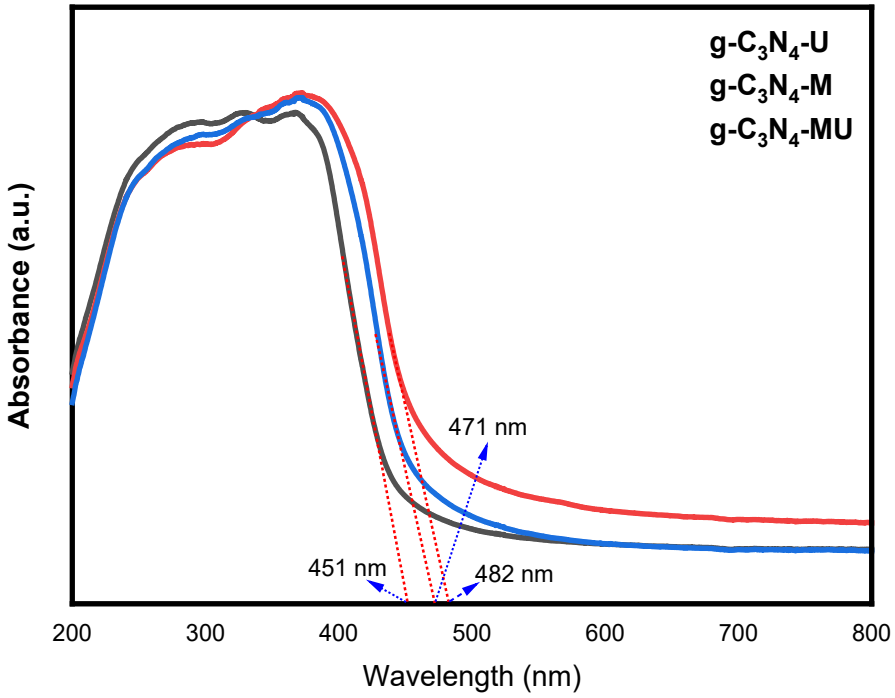

Fig. 3: UV-visible analysis of g-C_3N_4-U, g-C_3N_4-M, and g-C_3N_4-MU samples.

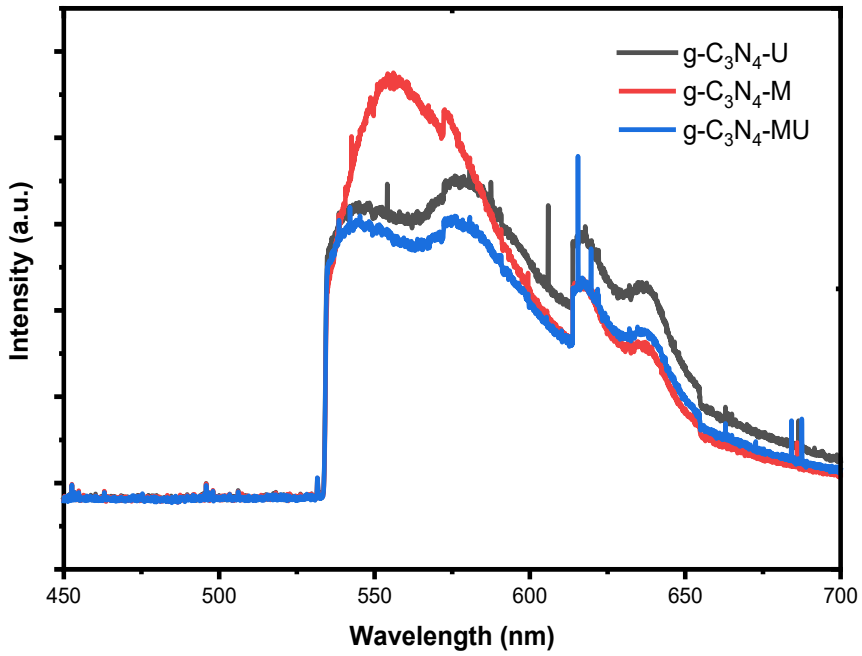

Fig. 4: Photoluminescence (PL) analysis of g-C_3N_4-U, g-C_3N_4-M, and g-C_3N_4-MU samples.

3.3. Photoluminescence (PL) Analysis

Photoluminescence (PL) analysis was carried out to further investigate the performance of the newly synthesized materials for charge carrier separation. A detailed grasp of photoluminescence is necessary to comprehend the creation and separation of photoinduced charges inside the semiconductor surface. The rate of electron and hole recombination and the performance of the photocatalytic process are inversely associated with the intensity of the PL spectrum [14]. Fig. 4 displays the PL spectra for the g-C_3N_4-M, g-C_3N_4-U, and g-C_3N_4-MU samples. In the case of g-C_3N_4-M, a higher recombination rate of charges was observed, as evidenced due to higher PL intensity. This was possibly due to the complete conversion of melamine to bulk g-C_3N_4 without any change in structure or the presence of surface defects. However, a lower PL intensity was achieved when urea was used as the precursor. This decrease in PL intensity was possible due to the presence of other materials in g-C_3N_4, which has provided forces to prevent charge recombination. Promising results in charge separations were obtained for the sample g-C_3N_4-MU, synthesized using a mixture of melamine and urea. This was possibly due to the presence of surface defects in the texture of g-C_3N_4, which have trapped electrons, thus preventing their recombination [19]. Due to the quantum confinement effect in nanotextures, g-C_3N_4-MU has lower PL intensity than g-C_3N_4-M and g-C_3N_4-U samples [16]. This demonstrates that the approach of inducing defects can trap electrons, preventing the recombination of photoinduced electrons, and would be beneficial to promote photocatalytic performance.

4. Conclusion

Defective graphitic carbon nitride (g-C_3N_4) was successfully synthesized and characterized using XRD, UV-visible, and PL techniques. Using melamine, g-C_3N_4-M was successfully synthesized, however, it exhibited lower photoinduced charge separation ability. Compared to g-C_3N_4, g-C_3N_4-U was found to perform better in charge separation, but it has a lower ability for visible light absorption. Comparatively, defective g-C_3N_4-MU synthesized using the mixture of melamine and urea had the highest ability for visible light absorption with promising charge carrier separation. These results show that low cost and highly efficient g-C_3N_4 can be synthesized using a simple single-step approach. The findings of this work would be promising for the field of photocatalytic CO_2 reduction, water splitting for hydrogen production, degradation, and other solar energy conversion applications.

Acknowledgements

This work was supported under research grants no. G00003296 and G00003501 from the National Water and Energy Center, United Arab Emirates University.

References

[1] H. Wang, X. Li, X. Zhao, C. Li, X. Song, P. Zhang, P. Huo, X. Li, A review on heterogeneous photocatalysis for environmental remediation: From semiconductors to modification strategies, Chin. J. Catal., 43 (2022) 178-214.

[2] M. Tahir, A.A. Khan, S. Tasleem, R. Mansoor, A. Sherryna, B. Tahir, Recent advances in titanium carbide MXene-based nanotextures with influential effect of synthesis parameters for solar CO2 reduction and H2 production: A critical review, Journal of Energy Chemistry, 76 (2023) 295-331.

[3] B. Tahir, M. Tahir, N.A.S. Amin, Ag-La loaded protonated carbon nitrides nanotubes (pCNNT) with improved charge separation in a monolithic honeycomb photoreactor for enhanced bireforming of methane (BRM) to fuels, Appl. Catal., B, 248 (2019) 167-183.

[4] Y. He, G. Jiang, Y. Jiang, L. Tang, C. Zhang, W. Guo, F. Li, L. You, S. Li, X. Liu, In-situ nanoarchitectonics of noble-metal-free g-C_3N_4@C-Ni/Ni_2P cocatalyst with core-shell structure for efficient photocatalytic H_2 evolution, J. Alloys Compd., 895 (2022) 162583.

[5] M. Tahir, B. Tahir, In-situ growth of TiO_2 imbedded $Ti_3C_2T_A$ nanosheets to construct PCN/$Ti_3C_2T_A$ MXenes 2D/3D heterojunction for efficient solar driven photocatalytic CO_2 reduction towards CO and CH_4 production, J Colloid Interface Sci, 591 (2021) 20-37.

[6] Z. Chen, F. Guo, H. Sun, Y. Shi, W. Shi, Well-designed three-dimensional hierarchical hollow tubular g-C_3N_4/$ZnIn_2S_4$ nanosheets heterostructure for achieving efficient visible-light photocatalytic hydrogen evolution, J Colloid Interface Sci, 607 (2022) 1391-1401.
[7] M. Tahir, Investigating the Influential Effect of Etchant Time in Constructing 2D/2D HCN/MXene Heterojunction with Controlled Growth of TiO_2 NPs for Stimulating Photocatalytic H_2 Production, Energy & Fuels, 35 (2021) 6807-6822.
[8] Y. Zhu, X. Zhong, X. Jia, J. Yao, Bimetallic Ni-Co nanoparticles confined within nitrogen defective carbon nitride nanotubes for enhanced photocatalytic hydrogen production, Environ. Res., 203 (2022) 111844.
[9] S. Zhu, Y. Cui, X. Wang, Y. Liu, W. Chen, Y. Zhang, Q. Wang, TiO_2 NTAs decorated with thin $CuBi_2O_4$ nanosheets for efficient photocatalytic dye degradation and hydrogen generation, Ceram. Int., 48 (2022) 6627-6637.
[10] H. Zhao, H. Fu, X. Yang, S. Xiong, D. Han, X. An, MoS_2/CdS rod-like nanocomposites as high-performance visible light photocatalyst for water splitting photocatalytic hydrogen production, Int. J. Hydrogen Energy, 47 (2022) 8247-8260.
[11] M. Tahir, A. Sherryna, A.A. Khan, M. Madi, A.Y. Zerga, B. Tahir, Defect Engineering in Graphitic Carbon Nitride Nanotextures for Energy Efficient Solar Fuels Production: A Review, Energy & Fuels, (2022).
[12] W. Xing, Y. Zhang, J. Zou, T. Zhang, C. Liu, G. Wu, G. Chen, Sulfur-doped 2D/3D carbon nitride-based van der Waals homojunction with superior photocatalytic hydrogen evolution and wastewater purification, Int. J. Hydrogen Energy, 47 (2022) 12559-12568.
[13] Y. Lu, W. Wang, H. Cheng, H. Qiu, W. Sun, X. Fang, J. Zhu, Y. Zheng, Bamboo-charcoal-loaded graphitic carbon nitride for photocatalytic hydrogen evolution, Int. J. Hydrogen Energy, 47 (2022) 3733-3740.
[14] Z. Zhang, Y. Zheng, H. Xie, J. Zhao, X. Guo, W. Zhang, Q. Fu, S. Wang, Q. Xu, Y. Huang, Synthesis of g-C_3N_4 microrods with superficial C, N dual vacancies for enhanced photocatalytic organic pollutant removal and H_2O_2 production, J. Alloys Compd., 904 (2022) 164028.
[15] X. Wang, Q. Li, Q. Lin, R. Zhang, M. Ding, CdS-sensitized 3D ordered macroporous g-C_3N_4 for enhanced visible-light photocatalytic hydrogen generation, J. Mater. Sci. Technol., 111 (2022) 204-210.
[16] X. Wang, Q. Li, L. Gan, X. Ji, F. Chen, X. Peng, R. Zhang, 3D macropore carbon-vacancy g-C_3N_4 constructed using polymethylmethacrylate spheres for enhanced photocatalytic H_2 evolution and CO_2 reduction, J. Energy Chem., 53 (2021) 139-146.
[17] Y. Zhou, M. Sun, T. Yu, J. Wang, 3D g-C_3N_4/WO_3/biochar/Cu^{2+}-doped carbon spheres composites: Synthesis and visible-light-driven photocatalytic hydrogen production, Materials Today Communications, 30 (2022) 103084.
[18] Y. Li, Z. Liu, Z. Li, Q. Wang, Renewable biomass-derived carbon-supported g-C_3N_4 doped with Ag for enhanced photocatalytic reduction of CO_2, J Colloid Interface Sci, 606 (2022) 1311-1321.
[19] T. Zhang, W. Wang, F. Gu, W. Xu, J. Zhang, Z. Li, T. Zhu, G. Xu, Z. Zhong, F. Su, Enhancing the low-temperature CO2 methanation over Ni/La-CeO2 catalyst: The effects of surface oxygen vacancy and basic site on the catalytic performance, Appl. Catal., B, 312 (2022).